

# Decoupled & Performance Analysis of 12/14 Bearingless Switched Reluctance Motor under Rotor Eccentricity faults

Nageswara Rao Pulivarthi\*, G.V. Siva Krishna Rao\*\*  
and G.V. Nagesh Kumar\*\*\*

## ABSTRACT

In this paper a decoupled nature of 12/14 bearing less switched reluctance motor (BSRM) based on FEM analysis and its performance analysis under rotor asymmetric faults are presented. The presence of decoupled nature between stator torque and suspension force in BSRM has a lead for operating with a simple PID controller. Asymmetric faults on rotor causes acoustic noise and vibrations in BSRM, and also effects the performance of the motor. To get decoupling nature, the motor torque winding and suspension force windings are independently placed on stator poles. At different currents and at different eccentric faults, flux linkages, inductances of both suspension and torque windings are observed. The radial force and motor torque along with its relative percentage ratio also observed for different rotor displacement faults. Among all the asymmetric faults, mixed eccentricity faults causes more impact on performance of motor. The analysis part of all these are carried out in 2-D FEM based MagNet software. Finally, this research gives a fruitful information regarding decoupling nature between suspension force and torque and rotor eccentric faults.

*Index Terms:* Bearing less, SRM, Decouple, Radial Force, Torque, Rotor Eccentricity, Mixed Eccentricity, MagNet

## 1. INTRODUCTION

Bearing less Switched Reluctance Motor had a extensive range of applications in modern world, as an electric vehicles, ventilators for the wind turbines and so on. This machine is more rugged, low cost, simple structure and more robustness as compare with other electrical magnetic bearing machines. The bearing less SRM has the benefits of no friction, no maintenance problem, no lubrication, and ultra-high speed operation.

The 8/6 BSRM model first introduced by M Takemoto, Suzuki and Akira Chiba in which motor torque and suspending forces are coupled each other, hence the controlling problem has increased while operating this conventional drive [1-3]. To get the decouple nature between suspending Force and motor torque, a single layer winding on single pole design was proposed by H. J. Wang, Dong. H. Lee and Jin Woo Ahn. A separate winding to suspension force and torque production purposes which are wound on separate salient poles. The same was applied to in this particular 10/8 and 12/14 BSRM [4-7]. An attractive radial force will build up between rotor and stator poles due to its saliency nature between stator poles and rotor poles [8-10]. This produced radial force can be further distributed into two components, one is suspension force component in x-y direction and other one is motor torque component. The x-y directional force component useful for levitate the rotor towards desired center position (0, 0) in x-y coordinate system. The motor torque component is useful for the rotation of rotor in radial direction[11-16].

\* Department of EEE Assistant Professor GITAM University, Email: [nnagesh@gitam.edu](mailto:nnagesh@gitam.edu)

\*\* Professor, Dept. of Electrical Engg. Andhra University, A.U.C.E, Email: [gvskrishna\\_rao@yahoo.com](mailto:gvskrishna_rao@yahoo.com)

\*\*\* Professor, Department of EEE GITAM University, Visakhapatnam, Email: [gundavarapu\\_kumar@yahoo.com](mailto:gundavarapu_kumar@yahoo.com)

This paper consists of a 12/14 BSRM which designed in MagNet 2D FEM based software. There are two kinds of windings on stator, and rotor does not carry any windings on it. Four suspension coils are chosen coordinately on stator frame so as to produce useful suspending force in X-Y direction to levitate the rotor in center position, and remaining eight torque coils are chosen diagonally on stator, to produce rotational torque. There are four poles are chosen under each phase, those are named as phase A and phase B. All six phases are energized individually by DC supply to get the decouple nature.

At first the decoupling between motoring torque and suspension force was observed with different currents of suspension winding, keeping motor torque winding currents are fixed at one value, similarly for second case with different currents of torque winding keeping suspension winding currents are fixed at one constant value. In first case the torque produced is not function of suspension force winding currents, and in second case, the suspending force produced from suspending winding is very less dependency of change of torque winding currents. To detect the short flux paths without flux reversal in torque coil phases, the distribution of flux configuration of proposed model was shown in fig.2, when both types of windings are excited at the same instant at different rotation angles.

The performance analysis of the motor under rotor eccentric displacements in which rotor is displaced only in Y-axis is done. The analysis is done for different values of current and rotor eccentric displacements by changing the rotor eccentricity. The main winding inductance, suspension force winding inductance, suspension force and torques are changed continuously and the performance of BSRM was descend at different rotor eccentricities. The performance analysis is done for flux linkages, radial forces and static torque characteristics under static, dynamic and mixed eccentricities. The better analysis leads to simple control and less vibration of BSRM.

## 2. DESIGN AND MODELLING OF PROPOSED 12/14BSRM

The total magnetic flux produced from the stator windings can be computed by the equation.

$$\oiint (B.n)ds \quad (1)$$

In which  $n$  is normal to surface  $\bar{s}$  and  $B$  is total magnetic flux density (Tesla).

The phase currents applied is 
$$I_{ph} = \frac{1}{R_{ph}} \left[ V_{ph} - \frac{d\phi(i, \theta)}{dt} \right] \quad (2)$$

Where  $R_{ph}$  is the resistance of the winding,  $v$  is the D.C voltage source and  $\theta$  is the rotor angular position. The inductance in each Phase, when ignoring saturation effect in both stator and rotor poles and fringing effects is denoted as:

$$L = \frac{\mu_0 N^2 L_{STK} R}{g} (\theta_0 + K_{fr}) \quad (4)$$

Subsequently, the motor torque ( $T$ ) produced in Phase is given as follows:

$$T = \frac{1}{2} i^2 L, \text{ n-mt} \quad (5)$$

The net suspending force produced both in x-y coordinate directions are written for proposed BSRM is given by

$$\begin{bmatrix} F_x \\ F_y \end{bmatrix} = \begin{bmatrix} K_{Fx} & 0 \\ 0 & K_{Fy} \end{bmatrix} \begin{bmatrix} i_x \\ i_y \end{bmatrix} \text{ Where } i_x = \begin{bmatrix} i_1^2 \\ i_3^2 \end{bmatrix} i_y = \begin{bmatrix} i_2^2 \\ i_4^2 \end{bmatrix} \quad (6)$$

A Novel 12 stator salient poles and 14 rotor salient poles of 12/14BSRM is designed and the fundamental model of the proposed 12/14BSRM is shown in the Fig 1. As shown from fig.1. The suspension Coil 3 and coil 1 used for control the suspension force in Y-directional, and coil 4 and coil 2 used for control the suspension force in X-directional. Coil 5 and coil 6 are named as phase-A and phase-B which produces a motoring torque. Due to symmetry of both torque phases, only one phase results are presented.

The design parameters of 12/14 Bearing less SRM is shown in Table 1.

<i>s. no</i>	<i>Parameters of BSRM</i>	<i>12/14 BSRM</i>
1	Stator Pole Number. ( $N_s$ )	12
2	Rotor pole Number. ( $N_r$ )	14
3	pole arc of Torque poles (deg) ( $B_t$ )	12.85
4	pole arc of Suspension poles (deg) ( $B_s$ )	25.71
5	pole arc of Rotor poles (deg) ( $B_r$ )	12.85
6	Axial stack length (mm)	40
7	stator Outer diameter (mm)	112
8	Rotor Outer diameter. (mm)	60.2
9	Stator Inner diameter. (mm)	7.7
10	Yoke thickness of Stator (mm)	0.3
11	Air gap thickness (mm)	18
12	Shaft Diameter (mm)	9.7
13	Number of turns on torque winding per pole	80
14	Number of turns on radial force winding per pole	100

To get eccentricity analysis results, the rotor's motion center is changed about 45% of its total air gap length. Here, we investigated the eccentricity of rotor in Y-direction only and there is no eccentric displacement in X-direction. The term is called the rotor radial displacement, in which value is positive when the rotor moves toward positive Y-axis and value is negative when the rotor displaces in the direction of negative Y-axis and is zero when the rotor is in geometrical center position.

### 3. FLUX DISTRIBUTION PATTERNS OF BSRM

Fig. 2. shows healthy condition i.e. no fault condition of proposed 12/14 BSRM when both windings are energized. From the fig. 2, we can observe that, short flux paths are not reversal in the motoring phase

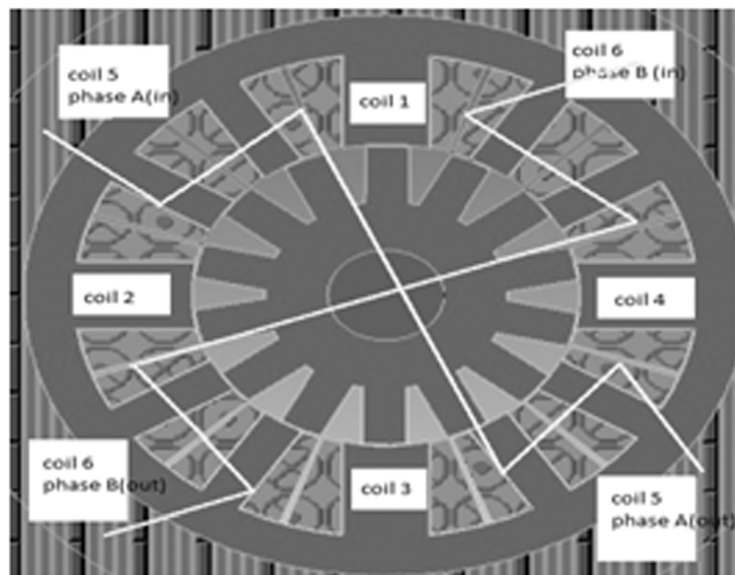


Figure 1: Proposed BSRM Model

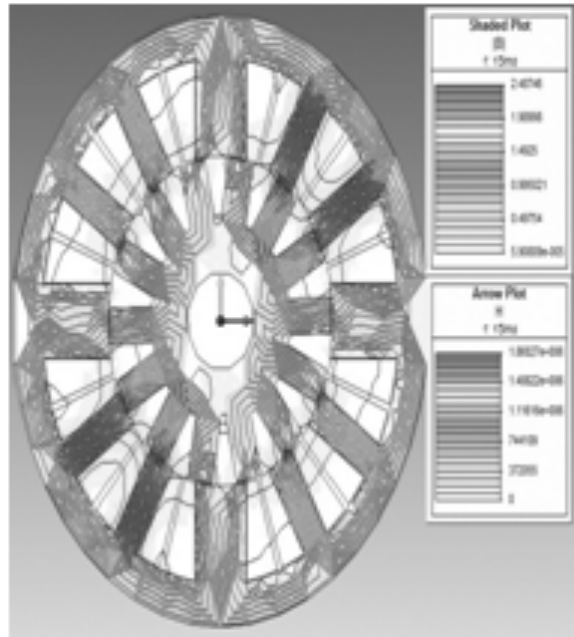


Figure 2: Healthy Condition

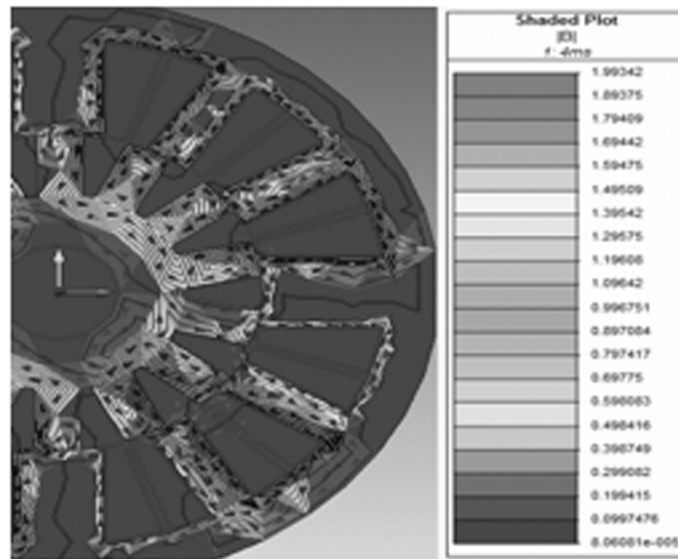


Figure 3: Flux distribution pattern at 0 Deg.

windings. The flux linkages of torque winding is more when the rotor pole is coincide with stator pole face, which is observed in Fig. 3, at rotor angular Position of 0 Deg.

## 4. DECOUPLE ANALYSIS

### 4.1. Torque and levitation winding flux linkages

The suspension force and torques are dependent on its own coil flux linkages. So, firstly we have to observe the flux linkages of both suspension force and torque coils with respect to rotor angular position. When the value of current is increasing then the flux linkages also increases, which is observed from fig. 4. (a) & 4 (b), similarly the flux linkages of torque windings Phase-A (coil-5) and Phase-B (coil-6) are also taken at different values of currents, which are shown in Fig. 4(c) & (d). From above plots, the flux linkages of torque coils phase A and phase B are excited at different time sequences, in order to keep a minimum reluctance path for rotation of rotor.

## 4.2. Levitation Forces versus control Current

The net value of force produced from suspension coils is directly proportional to suspension current, when the magnitude of current increases, the levitation force also increases, which is observed and shown in Fig. 5, at different values of control currents of coil 1&3. The resultant suspension force produced is same for both negative value of currents and positive values of currents (mirror image), hence it proves that suspension force is not dependent of polarity of a current.

## 4.3. Suspension Force with respect to Rotor Angular position

The suspension force produced from all coils is independent of rotor angular position and dependent on only its winding currents, which is observed and shown in fig. 6 (a) & (b). The suspension force is individually displayed for suspending force coils 2 & 4, 1 & 3. Fig. 6 (a) & (b) shows that, by increasing the magnitudes of control current, the suspension force of suspension coils also rises. All the suspending force coils are energized at the same time.

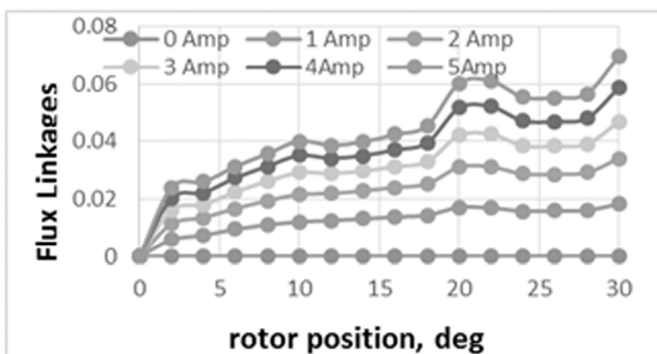


Figure 4 (a): Flux linkages of suspension coil-1

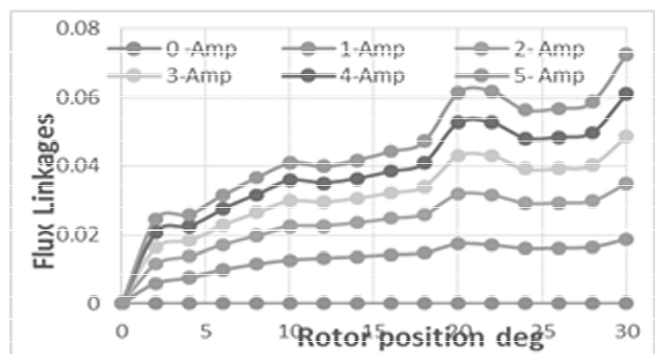


Figure 4 (b): Flux linkages of suspension coil-2

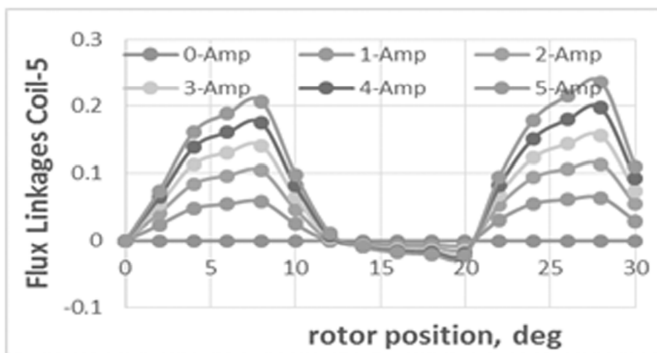


Figure 4 (c): Flux linkages of coil-5

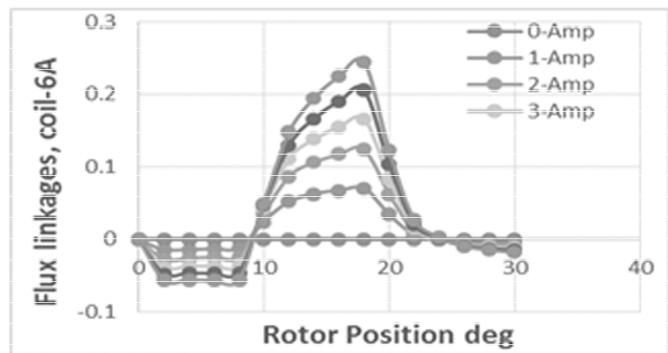


Figure 4 (d): Flux linkages of coil-6

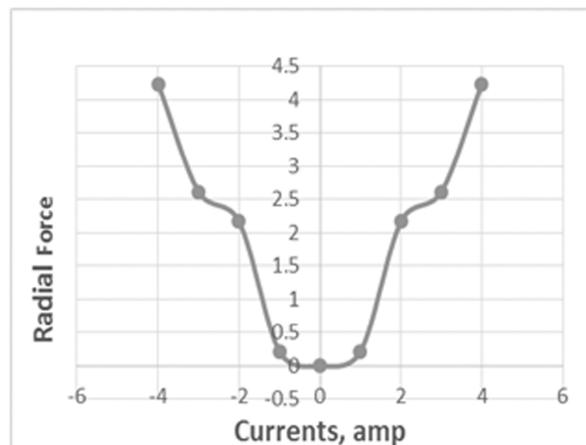


Figure 5: Suspension Force at different control currents

### 4.4. Net stator Torque profile

The Torque produced from stator coils, phase-A and Phase-B is function of angular position of rotor and winding current, which is observed and shown in fig. 7 at different values of phase currents at different rotor angular positions. With the similarity of all torque poles, here we considered the torque pole of Phase-A, to observe the torque profile at different currents with respect to angular position of rotor.

From fig. 7. it shows that the Static torque value is gradually increases up to 7-degrees and again these

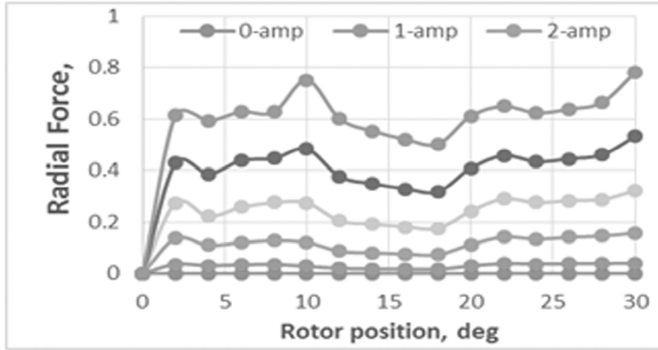


Figure 6 (a): Suspension Force of suspension coil-1

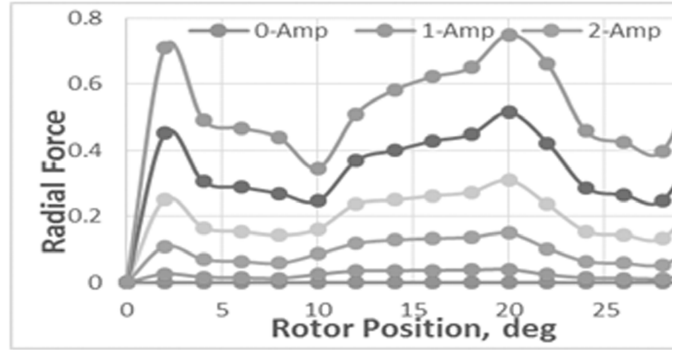


Figure 6 (b): suspension Force of suspension coil- 2.

value is decreases and reaches to minimum value nearly to 0.2(N-mt) up to 13 degrees. From the fig.7, it is decided that, whenever the edge of the rotor pole approach towards stator pole, the stator torque produced from the two phases will be maximum and the maximum value increases with the increase of current.

### 4.5. Suspending force & Torque decoupled characteristics

To observe the decoupling nature between suspension force and torque, at first, the values of suspension winding currents are varied keeping currents of torque coil as constant, this can be observed from fig.8. Similarly by varying currents of torque coils and keeping suspension winding currents as constant, which is also observed and shown in, fig. 9 it is clear that by varying suspension winding force current there is a very little change in torque, it is due to mutual inductance between suspension force and motoring torque windings. From fig. 9, the effect of torque current on suspension force is small, hence the torque currents has almost zero effect on suspension force and vice versa. From the directly above study it may be decided that suspension force control is decoupled from control of stator torque in proposed 12/14 BSRM model.

## 5. PERFORMANCE ANALYSIS OF BSRM UNDER ROTOR ECCENTRIC DISPLACEMENTS:

### 5.1. Windnding Inductances at healthy&faulty condition

The high speed operation of BSRM depends upon exact control of currents both in torque and suspension force windings. These currents will affect the inductance of both torque and suspension windings. From

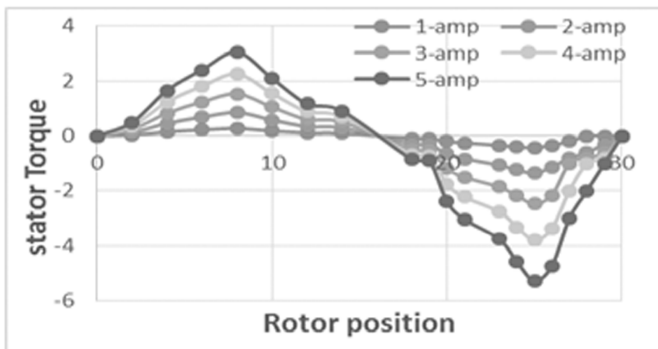


Figure 7: Stator torque

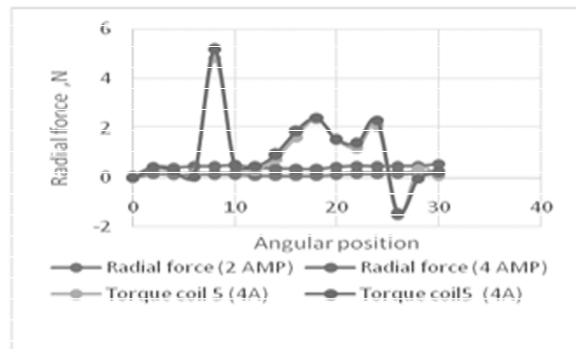


Figure 8: Torque and suspension force profile

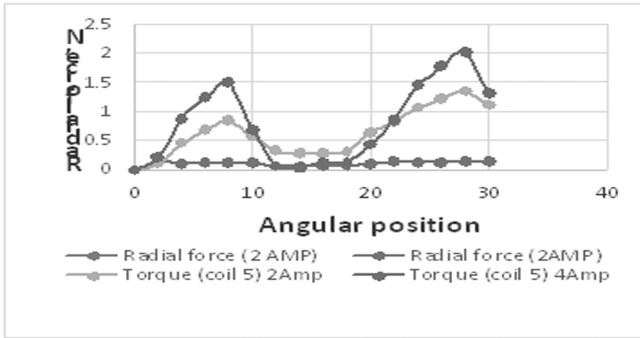


Figure 9: Torque W.r.t. Suspension force.

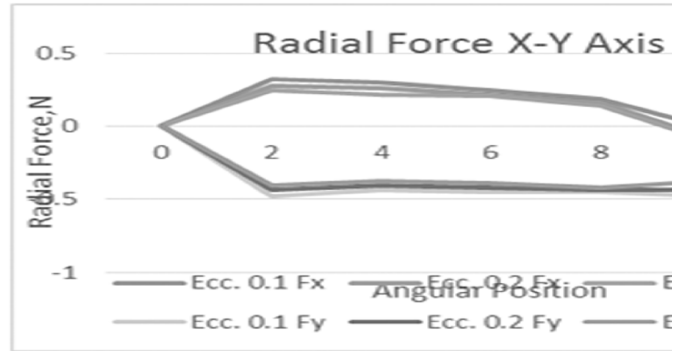


Figure 10: Decoupling nature between Fx and Fy:

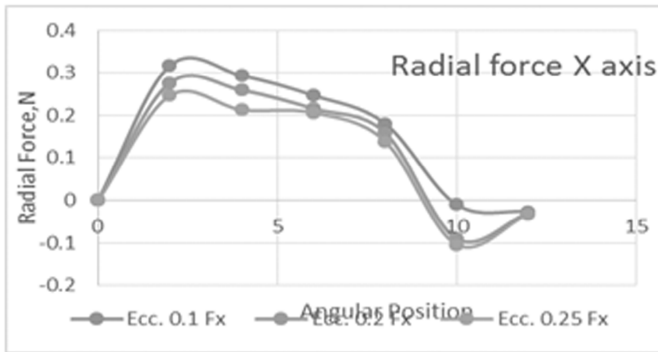


Figure 11: Decoupling between Fx and Fy:

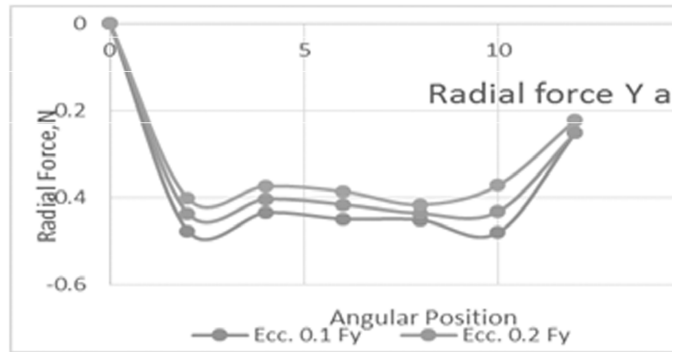


Figure 12: Decoupling between Fx and Fy:

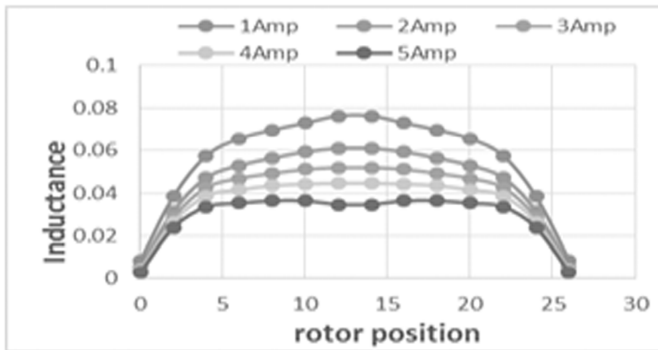


Figure 13: Main torque winding inductances

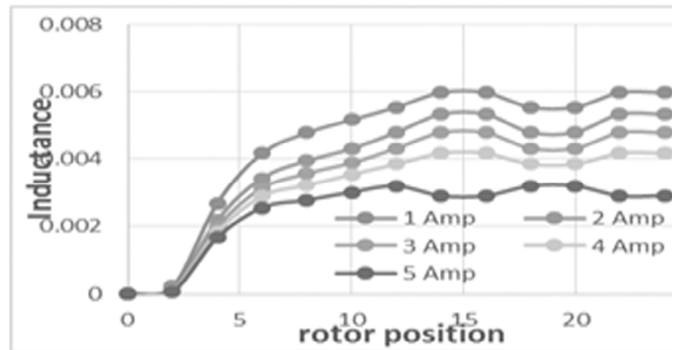


Figure 14: Suspension winding inductances

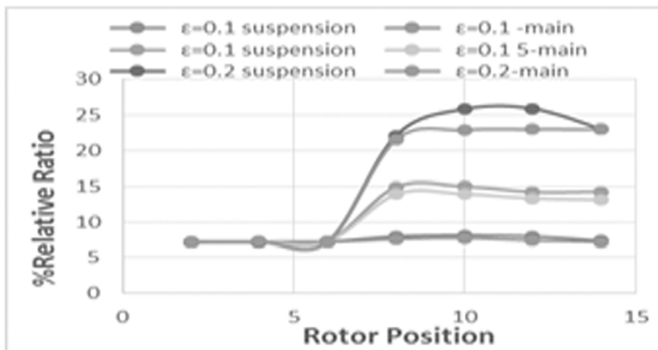


Figure 15: Winding inductance at different Eccentricity.

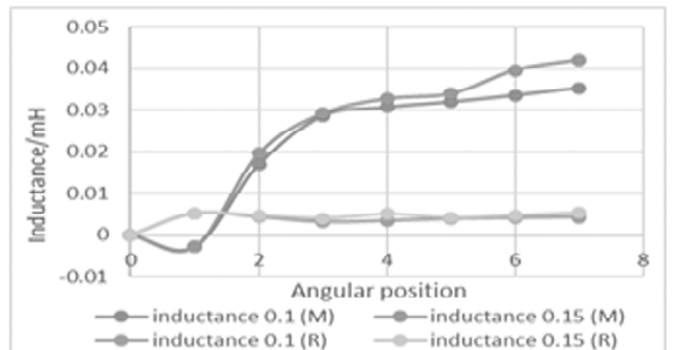


Figure 16: Relative change ratio % at different Eccentricity.

fig13&14, the inductances of main and suspension windings at different values of control currents are taken when the rotor is at geometric centre, when increasing control currents in both main torque winding and suspension winding.

**Table 2**  
**Fault definitions for implementation purposes.**

<i>Fault type</i>	<i>Rotor displacement</i>	<i>Motion center</i>
DE	(0,R,0)	(0,0,0)
SE	(0,R,0)	(0,R,0)
ME	(0,R/2,0)	(0,R/2,0)

When the main winding current,  $I_m = 15A$  and suspension winding current is  $I_s = 8A$  at different positive eccentric displacements  $\epsilon = 0.1mm$  and  $\epsilon = 0.15mm$ , the winding inductances are calculated and shown in fig. 15. The percentage of relative change ratio between main winding inductance and suspension winding inductance are also shown in fig.16. The net inductances of main and suspension force windings, and their percentage of relative change ratio rises with the increase of eccentric radial displacement. It is concluding that eccentricity has a strong influence on winding inductances.

**5.2. Suspension Force and Static Torque profile at healthy and faulty conditions**

The positive eccentric displacements have more impact on motor performance parameters like suspension force and torque of main winding, as compare with negative eccentric displacements. The radial force and main winding torque performance is verified and shown in Fig. 17 & Fig. 18 respectively. The values of both positive and negative displacement increases, the radial force percentage will also increase. From Fig.18, when the eccentricity is zero the torque values lies in the middle and by increasing eccentricity displacement in positive Y-directional, the torque value is increases and vice versa. The relative change ratio of torque which increases by increasing the value of eccentricity fault values, this is shown in Fig.19&20

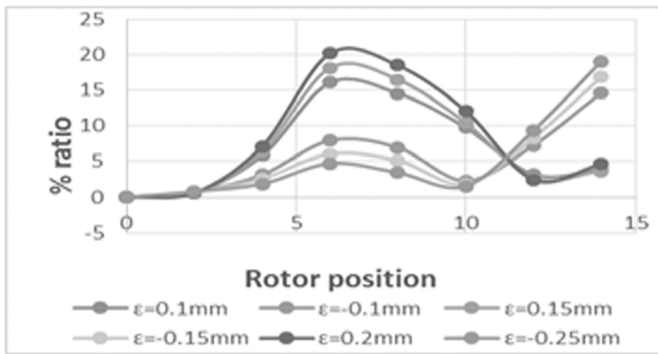


Figure 17: Radial force at different eccentricity

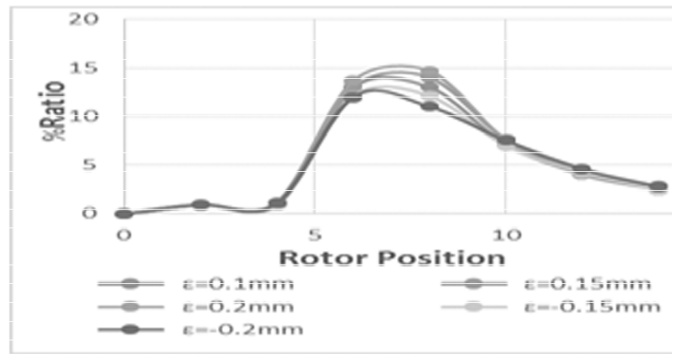


Figure 18: Relative percentage change ratio of Radial force

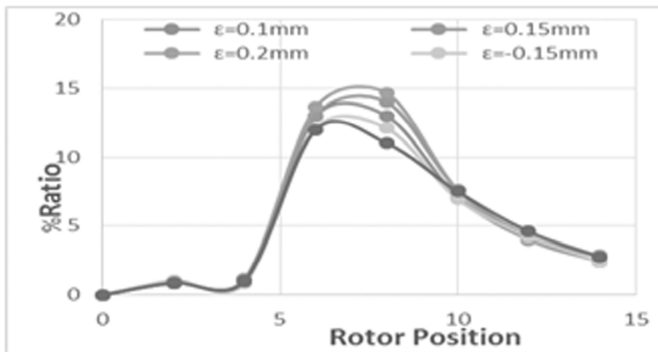


Figure 19: Torque at various eccentricity values

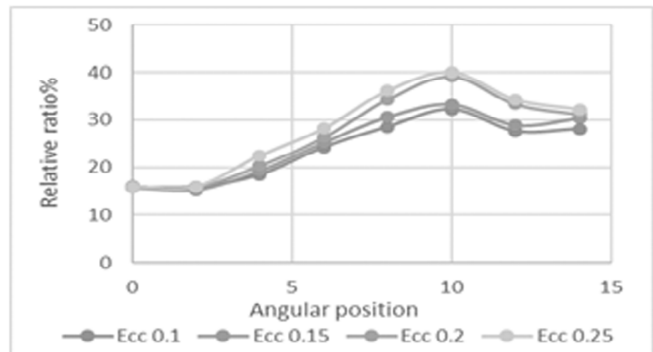


Figure 20: Relative percentage change ratio of torque



### 5.3. The suspension Force of suspension coils at different eccentricity faults

The radial forces of suspension coils are shown in Fig. 21 as a function of angular position the radial force is necessary to levitate the rotor and keeps at center position. The radial forces in SE and DE cases are almost similar. In case of ME, the radial force variations are high in which it leads to an uneven levitation force.

### 5.4. Static Torque Characteristics of BSRM at different eccentricity faults

The static torque is maximum when the rotor and stator teeth are coinciding together, this is observed in all the SE, DE, ME cases. The DE case shows the minimum variation and ME case shows the maximum variation in static torque. The fault severity is high in ME fault case as shown in Fig. 22.

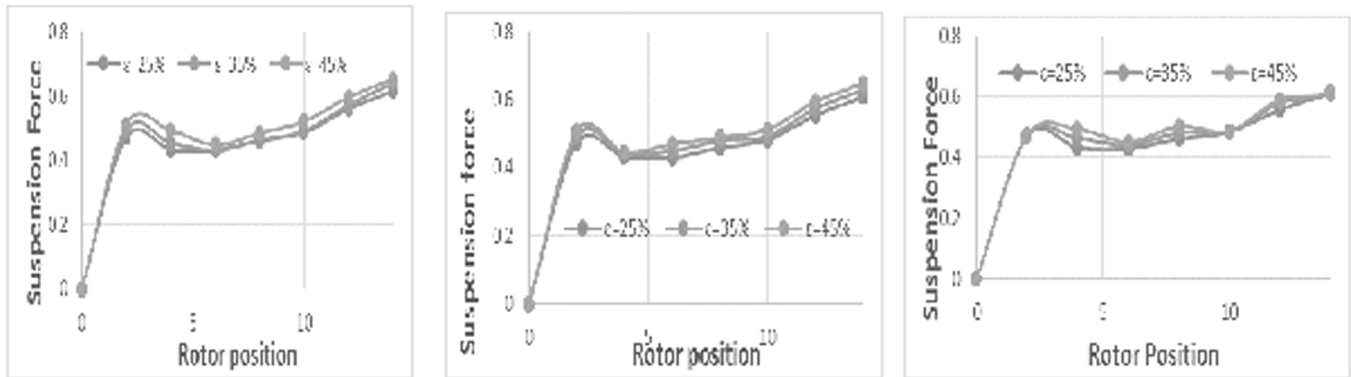


Figure 21: (a, b & c). Suspension Force of suspension Coils under S.E, D.E & M.E faults

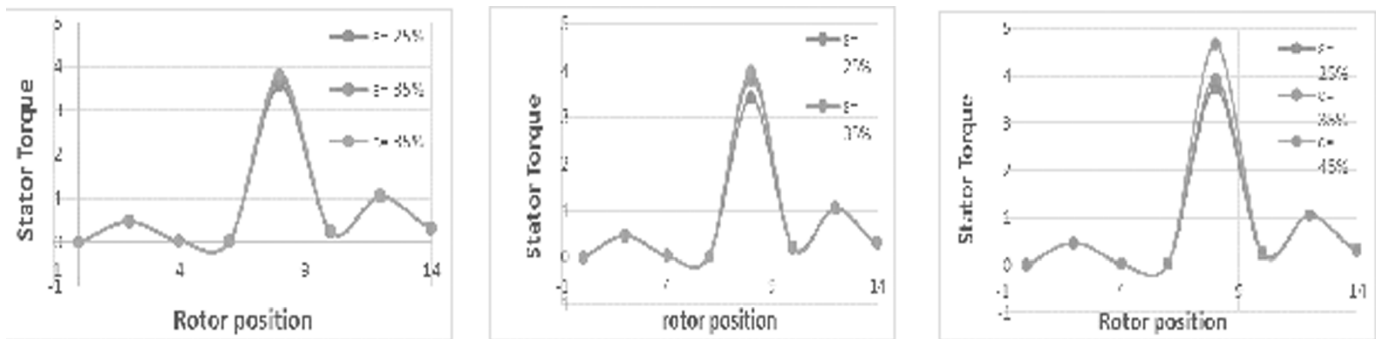


Figure 22: (a, b & c). Stator Torque of motor coils under S.E, D.E & M.E faults.

## 6. CONCLUSION

The decoupled nature among motor torque and suspension force and performance analysis under rotor eccentric faults for a 12/14 BSRM is observed. Through FEM analysis on 12/14 BSRM an excellent decoupling environment between stator torque control and suspension force control is found at different values of currents. The performance results of Bearing less switched reluctance motor in condition of rotor eccentric displacement and asymmetric rotor fault (SE, DE, ME) were compared for healthy condition. The Inductance values of both the windings are increased, when there is an increase of rotor eccentric displacements. Suspension force and motor torque increases, when there is an increase of rotor eccentric displacements in Y-direction. Rotor eccentric displacements have a significant effect on the performance of BSRM parameters. The flux linkages, suspension force and Static torque profile for changed percentages of SE, DE and ME are shown. From above results and discussions, we conclude that ME fault is more severe than DE and SE. This study leads to better control and fault diagnosis of BSRM and Experimental verification also.

**REFERENCES**

- [1] M. Takemoto, K. Shimada, A. Chiba and T. Fukao, "A design and characteristics of switched reluctance type bearingless motors," in Proc. 4th Int. Symp. Magnetic Suspension Technology, Vol. NASA/CP-1998-207654, pp. 49-63, May 1998.
- [2] M. Takemoto, K. Shimada, A. Chiba and T. Fukao, "A design and characteristics of switched reluctance type bearingless motors," in Proc. 4th Int. Symp. Magnetic Suspension Technology, Vol. NASA/CP-1998-207654, pp. 49-63, May 1998.
- [3] Takemoto M, Chiba A, Akagi H, Fukao T. Radial force and torque of a bearingless switched reluctance motor operating in a region of magnetic saturation. In: Proceeding of record IEEE industry applications society annual meeting; 2002. p. 35-42.
- [4] H. J. Wang, D. H. Lee and J. W. Ahn, "Novel Bearingless Switched Reluctance Motor with Hybrid Stator Poles: Concept, Analysis, Design and Experimental Verification," The Eleventh International Conference on Electrical Machines and Systems, 2008: 3358-3363
- [5] Zhenyao Xu, Dong-Hee Lee, Jin-Woo Ahn, "Modeling and Control of a Bearingless Switched Reluctance Motor with Separated Torque and Suspending Force Poles".
- [6] Zhenyao Xu, Fengge Zhang, Jin-Woo Ahn. "Design and Analysis of a Novel 12/14 Hybrid Pole Type Bearingless Switched Reluctance Motor"
- [7] Zhenyao Xu, Dong-Hee Lee, Jin-Woo Ahn, "Control Characteristics of 8/10 and 12/14 Bearingless Switched Reluctance Motor", the 2014 International Power Electronics Conference.
- [8] Li Chen, Wilfried Hofmann. Analytically computing winding currents to generate torque and levitation force of a new bearingless switched reluctance motor. In: Proceeding of the 12th international power electronics and motion control conference; 2006. pp. 1058-63.
- [9] Feng-Chieh Lin, Sheng-Ming Yang. An approach to producing controlled radial force in a switched reluctance motor. IEEE Trans Ind Electron 2006; 54(4):2137-46.
- [10] R. Krishnan, R. Arumugan, and J. F. Lindsay, "Design procedure for switched-reluctance motors," IEEE Trans. Ind. Applicat., vol. 24, pp. 456-461, May/June 1988.
- [11] Junfang Bao, Huijun wang, Bingkun Xue, "The Coupling Characteristics Analysis of a Novel 12/14 Type Bearingless Switched Reluctance Motor", 2014 17th International Conference on Electrical Machines and Systems (ICEMS), Oct. 22-25, 2014, Hangzhou, China.
- [12] Huijun Wang, Junfang Bao, Bingkun Xue and Jianfeng Liu, "Control of Suspending Force in Novel Permanent Magnet Biased Bearingless Switched Reluctance Motor", 2013 IEEE.
- [13] Bingkun Xue\*, Huijun Wang, Junfang Bao, "Design of Novel 12/14 Bearingless Permanent Biased Switched Reluctance Motor", 2014 17th International Conference on Electrical Machines and Systems (ICEMS), Oct. 22-25, 2014, Hangzhou, China.
- [14] [12] Hongyun Jia, Chao Fang, Tao Zhang, "Finite Element Analysis of a Novel Bearingless Flux Switching Permanent Magnet Motor With the Single Winding", 2014 17th International Conference on Electrical Machines and Systems (ICEMS), Oct. 22-25, 2014, Hangzhou, China.
- [15] [13] Han Yang, Zhiqian Deng, Xin Cao, Lei Zhang, "Compensation Strategy of Short-Circuit Fault for a Single-Winding Bearingless Switched Reluctance Motor", 2014 17th International Conference on Electrical Machines and Systems (ICEMS), Oct. 22-25, 2014, Hangzhou, China.
- [16] Junfang Bao, Huijun wang, Jianfeng Liu, et al. "self-starting analysis of a novel 12/14 type bearingless switched reluctance motor", proc. IEEEICIT, pp. 866-871, 2014.